Production of nanocrystalline TiB_2 powder through self-propagating high temperature synthesis (SHS) of TiO_2–H_3BO_3–Mg mixture

Saikumar Gadakary[1]*, Asit K. Khanra[1] and R. Veerabau[2]

Nanocrystalline TiB_2 powders are produced through self-propagating high temperature synthesis (SHS) technique by igniting the stoichiometric mixture of titanium oxide (TiO_2), boric acid (H_3BO_3) and magnesium (Mg) powder. Different percentages of NaCl are added to the mixture as SHS diluent in order to control the particle size of the TiB_2. The synthesised and purified powder is characterised by X-ray diffraction and electron microscopes respectively. The SEM images show the presence of agglomeration of fine spherical particles. The TEM images reveal the formation of nanocrystalline TiB_2 particles. The particle size is found to decrease with the addition of NaCl. The TEM images reveal the presence of crystallographic defects in the powder. In order to find out the reaction mechanism of TiO_2–H_3BO_3–Mg system, the synthesis of TiO_2–Mg and H_3BO_3–Mg mixtures is performed in inert atmosphere and phase analysis of TiO_2–Mg and H_3BO_3–Mg mixtures reveal the reaction mechanism.

Keywords: Ceramics, Nanocrystalline powders, Self-propagating high temperature synthesis, Titanium diboride, X-ray diffraction, Electron microscope

Introduction

Titanium diboride (TiB_2) is an advanced ceramic material. It has properties like high melting point (~3243 K), high hardness, low density, good elastic modulus, excellent mechanical properties, good thermal and electrical conductivity, and corrosion resistance properties etc.[1–3] TiB_2 has applications in rocket nose cone for atmospheric re-entry, ballistic armour, cathodes for Hall–Heroult cells, crucibles for molten metals, metal evaporation boats, coating on cutting tools.[4,5] It is widely used as cutting tool composites and wear resistance parts.[6] The TiB_2 powder is synthesised by different methods such as carbothermic reduction of TiO_2 and B_2O_3 mixture, gas phase Na/$TiCl_4$/BCl_3 flame reaction, direct reaction of Ti, its oxide and its hydrides with elemental boron, reaction of $NaBH_4$ and $TiCl_4$, reactions of elemental powders, solution phase processing route, gas phase combustion synthesis process, self-propagating high temperature synthesis (SHS),[7–10] laser melting,[11] ball milling,[12,13] and carbothermic reductions of metal oxide–boron oxide mixture.[14–16] There are research reports on mechanochemical and mechanical alloying route for the production of nanocrystalline TiB_2 powder.[17,18] Nozari *et al.* studied the mechanochemical behavior of TiO_2–B_2O_3–Si system to produce TiB_2 nanoparticles.[19]

In the present paper, the TiB_2 powder is synthesised by SHS method. The main feature of the SHS process is that, it utilises the high energy released during the exothermic chemical reaction of the reactants to yield a variety of inorganic materials. Once the reactants are ignited by an external source, the reaction front propagates within the solid with a certain velocity to complete the chemical reaction. The ignition time is very short and localised activation is sufficient, which enables the preparation of a large numbers of high temperature advanced materials without employing any high temperature furnaces. The SHS offers wide applications for manufacturing of several inorganic materials such as CrB, HfB,TiC, ZrC, HfC, Mg_3N_2, BN, hydrides, intermetallics, carbonitrides, cemented carbides, chalcogenides, binary compounds, and composites.[20] Self-propagating high temperature synthesis has a wide range of applications such as in abrasives, cutting tools, polishing powders, resistive heating elements, shape memory alloys, high temperature intermetallic compounds, etc.[20] Self-propagating high temperature synthesis method is also developed to be used in preparing dense ceramics and glasses by melt casting instead of conventional powder sintering.[21,22] This technique combines strong exothermic chemical reactions with a high gravity field, and offers an efficient and furnace free way for rapid production of bulk ceramic and glass materials. The main drawbacks of this process are to control the kinetic of reaction because of very fast process. There are few research papers which deals with kinetic study SHS process. The SHS of elemental Ti and B leads to formation of high pure TiB_2 powder. However, the use of elemental mixture results in increase in production cost. In the present investigation, an attempt

[1]Department of Metallurgical and Materials Engineering, National Institute of Technology, Warangal, Telangana, India
[2]Defence Metallurgical Research Laboratory, Kanchanbagh, Hyderabad, India

*Corresponding author, email sai.gadakary@gmail.com

Published by Maney on behalf of the Institute
Received 28 April 2014; accepted 29 June 2014
DOI 10.1179/1743676114Y.0000000188

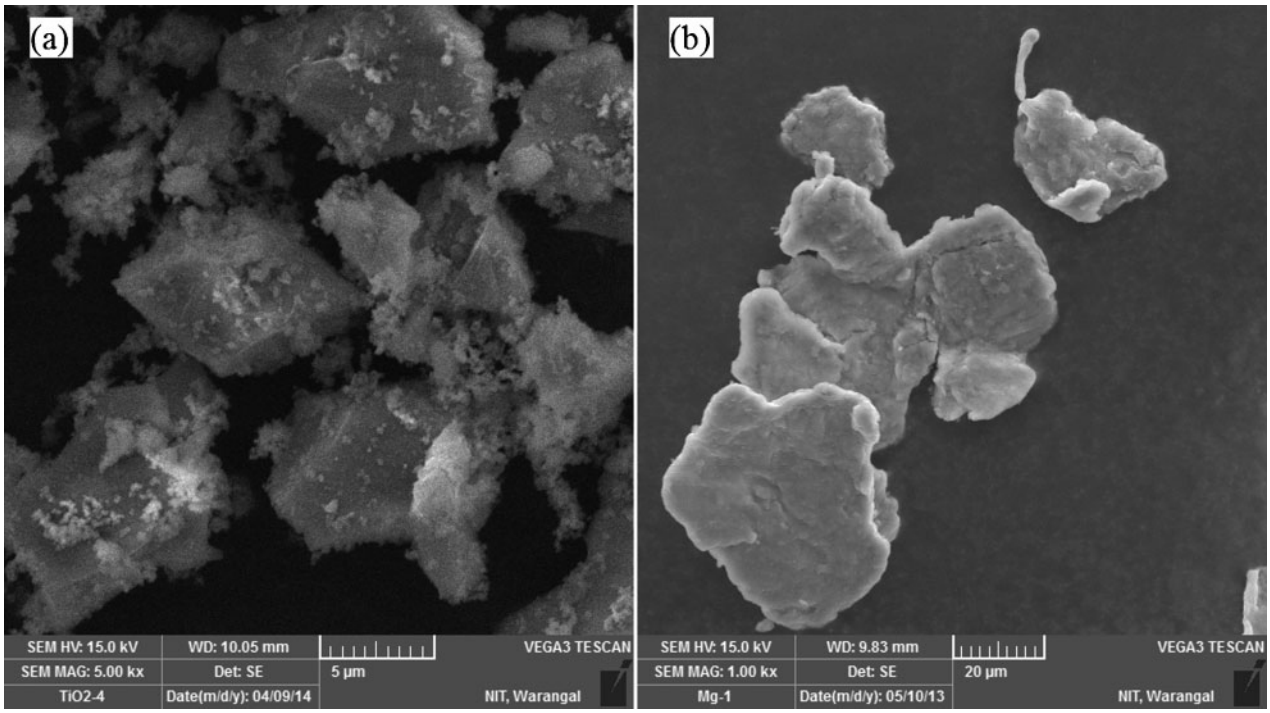

a TiO_2; *b* Mg powder

1 Micrographs (SEM) of raw materials

has been taken to produce the TiB_2 powder by SHS of alternative materials to decrease the production cost and study the kinetic of the process. The different morphology of TiB_2 particles are produced by controlling the process parameters. The synthesised powder is characterised by X-ray diffraction (XRD) and electron microscopes, etc.

Experimental procedure

Materials

Titanium oxide (TiO_2) (>99·9% pure, Loba Chemicals, India), boric acid (H_3BO_3) (99·9% pure, Loba-Chemicals, India) and magnesium (99·9% pure and

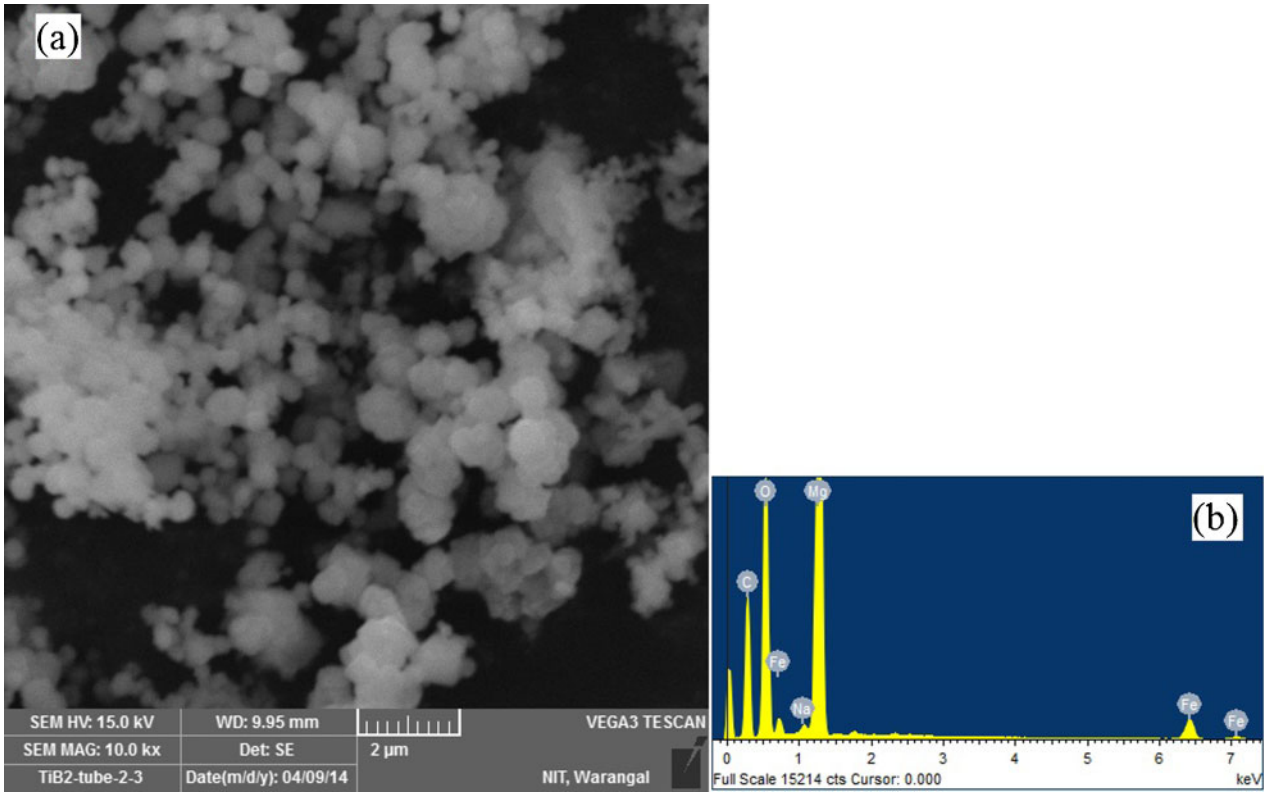

a SEM image of powder; *b* EDS of powder

2 Morphology under SEM of white powder collected at walls of tube

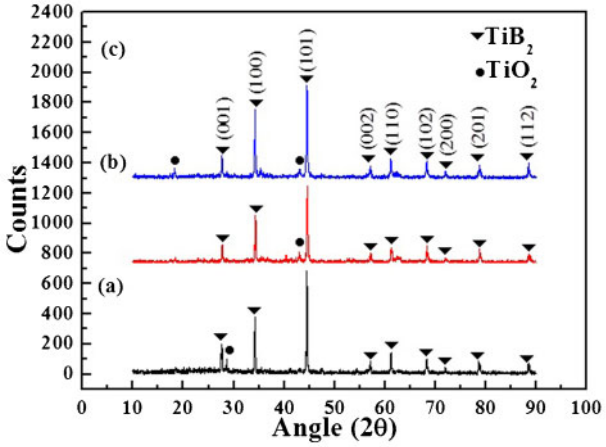

a sample A; *b* sample B; *c* sample C

3 Patterns (XRD) of different samples

particle size <150 μm, Loba-Chemicals) were used for the synthesis of TiB_2.

Experimental procedure

The mixture of titanium oxide (TiO_2), boric acid (H_3BO_3) and magnesium was taken as per the stoichiometric reaction (equation (1)). The powders were mixed in a mortar mixer for about 20 min. A mixture of 20 g was then taken in a stainless steel boat and was kept in a tubular furnace (Inconel tube; Systems control, Chennai, India). The total process was carried out in the high pure argon atmosphere in order to maintain an inert atmosphere. The furnace was then heated up to 800°C, with a constant heating rate. It was observed that the reaction was taking place with explosive sound at an approximate temperature of 680±15°C. The furnace is then left for cooling to room temperature.

$$TiO_2\ (s) + 2H_3BO_3\ (s) + 5Mg\ (s) \rightarrow TiB_2\ (s) + MgO\ (s) + 3H_2O\ (g) + \Delta H \quad (1)$$

After cooling, the synthesised powder was taken out. It was observed that the reacted mixture is formed of black lumps, and some amount of white layer is formed on the lumps. The powder is crushed into fine powder before the leaching process. The leaching process was carried out in diluted HCl with normality of 2 N. The solution was mixed with the crushed powder and heated up to 120°C. The process was continued till the solution boils for about 10 min, and then the solution was separated by using the filter paper. The resulting powder, which was taken after leaching process, was then dried in an oven for 1 h. The resultant powder was subjected to further characterisation.

The process was also carried out with an addition of different weight percentages of NaCl as a SHS diluent. The NaCl is added with weight percentages of 10 and 20 wt-% respectively. The phase analysis of the

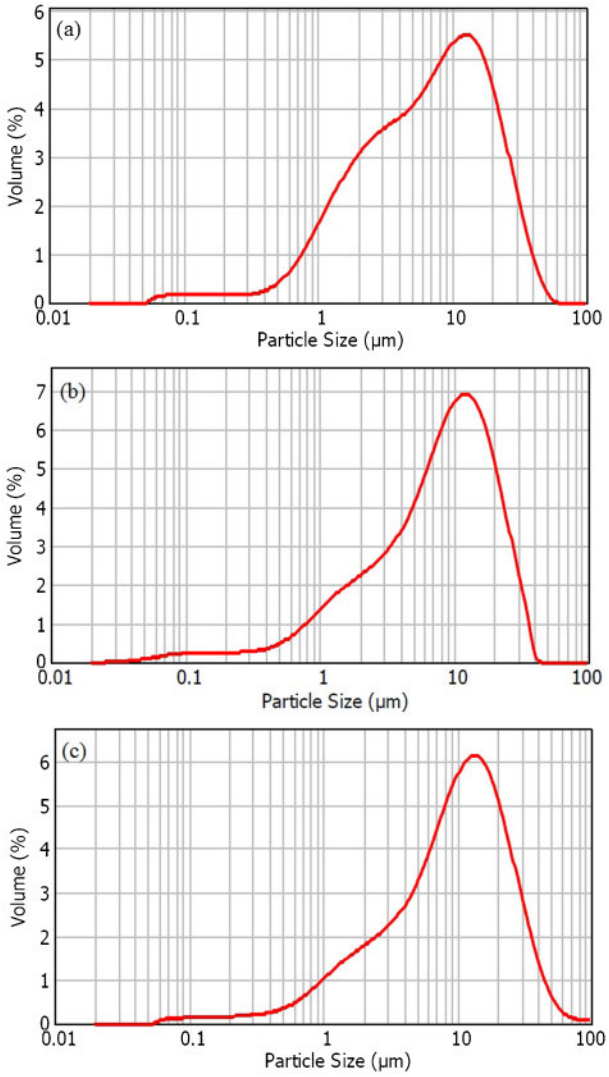

4 Particle size distribution of SHS synthesised *a* TiB_2, *b* TiB_2 added with 10 wt-% of NaCl, and *c* TiB_2 added with 20 wt-% of NaCl

synthesised powder was carried out by using an X-ray diffractometer with Cu K_α (λ=1·54 Å) radiation (Philips X-ray diffractometer, PW1730). The particle size analysis of different samples was determined by using particle size analyser (Malvern Instruments Ltd, UK) using laser scattering technique. During the particle size analysis, the powder was dispersed in alcohol. Morphology of the powder was analysed by a scanning electron microscope (SEM) (TESCAN, VEGA3 LMU VG9231273IN) and a transmission electron microscope (TEM) respectively. The SEM samples are prepared by dispersing the powders in methanol and dispersed by using ultrasonic cleaner. The sample is prepared by dropping the dispersed powder on the carbon tape. Samples for TEM examination were prepared initially by dispersing the powders in methanol using ultrasonic cleaner for 20–30 min. The particles were subsequently collected on the

Table 1 Effect of SHS diluent on crystallite size of TiB_2 powder

Sample no.	NaCl/wt-%	Angle (2θ)/°	Broadening (β)/°	Crystallite Size/nm
A	0	44·3	0·20	42
B	10	44·5	0·23	14
C	20	44·4	0·26	9

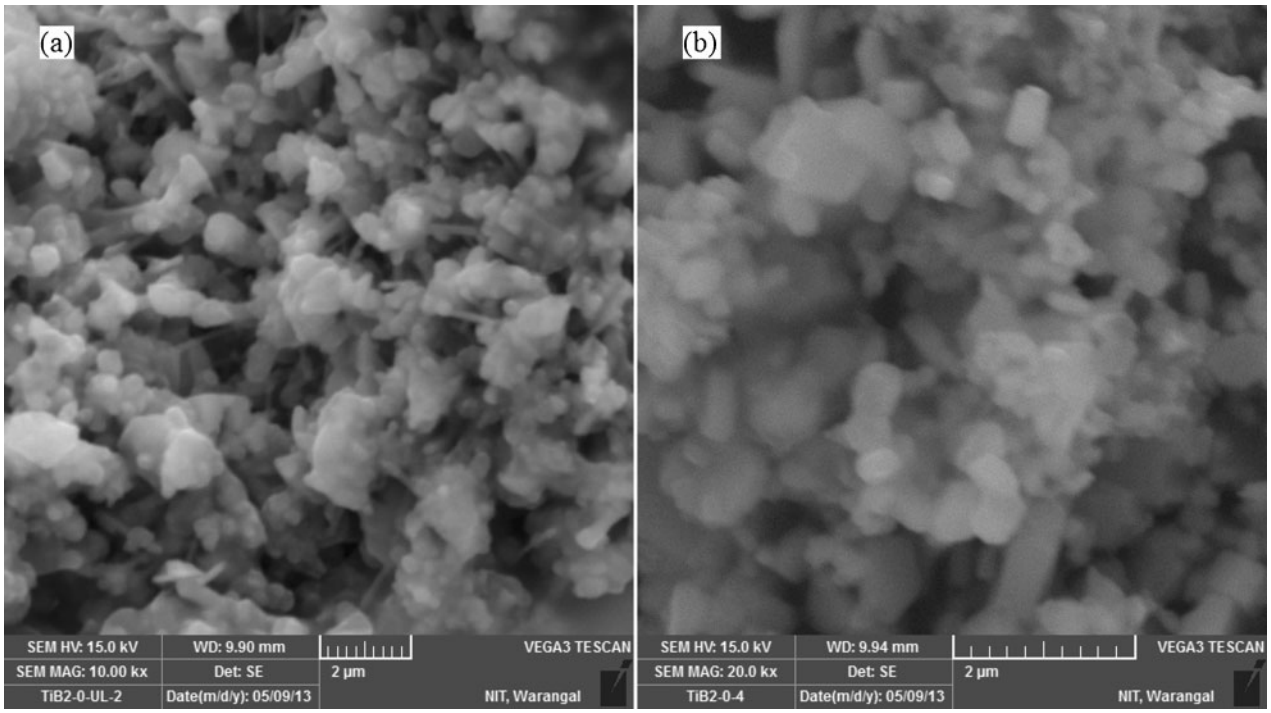

a unleached powder; *b* leached powder

5 Images (SEM) of sample A (0% NaCl)

carbon coated copper grids and the foils were allowed to dry under UV lamp. The TEM samples were examined under FEI make Tecnai G^2 transmission electron microscope equipped with energy dispersive X-ray spectroscopy (EDS) system. Scanning electron microscopy micrographs showing the morphology of Mg and TiO_2 powder are shown in Fig. 1. TiO_2 powder (Fig. 1*a*) reveals agglomeration of particles as big chunks, whereas Mg powder (Fig. 1*b*) shows the presence of flaky shaped particles with surface cracks.

To study the kinetics of the process of TiO_2–H_3BO_3–Mg system, the synthesis of individual mixture such as TiO_2–Mg and H_3BO_3–Mg was performed in an inert atmosphere. The as synthesised and leached powder was characterised by XRD.

Results and discussion

The as synthesised lumps were found in the tube and there was deposition of fine white powder on the tube wall. The colour of the lumps is black and most of the lumps are partially covered with fine white powder. The SEM image of fine white powder is shown in Fig. 2. It shows the presence of agglomerates of fine spherical particles. Energy dispersive X-ray spectroscopy analysis of the powder shows the presence of magnesium and oxygen along with other minor elements such as Fe and C. Since the lower atomic number elements cannot be detected reliably using EDS, the Mg peak indicates that these powders are essentially MgO phase. These lumps are ground and leached in dilute HCl for purification.

Phase analysis of synthesised powder

The XRD patterns of sample produced by SHS process using different amounts of NaCl are shown in Fig. 3. The phase analysis of leached powder shows presence of mainly TiB_2 as major phase with TiO_2 as minor phase in all the cases. The XRD patterns indicate extensive line broadening for the NaCl added samples. The broadening of 101 peaks (the highest intensity at 44·4°) of TiB_2 and the instrument line broadening of 0·2° is used for the calculation of average crystallite sizes, D using the Scherrer formula, (ignoring the defect or strain contribution)[23]

$$D = \frac{0{\cdot}9\lambda}{\beta_c(2\theta)\cos\theta} \tag{2}$$

where, $\beta_c(2\theta)$ is the corrected broadening of the diffraction line measured at half the maximum intensity for the peak that appeared at the Bragg angle 2θ and λ is the corresponding wavelength of the X-ray radiation. The line broadening is corrected by using the following expression[23]

$$\beta_c^2(2\theta) = \beta_o^2(2\theta) - \beta_i^2(2\theta) \tag{3}$$

In the above equation, $\beta_o(2\theta)$ is the observed line broadening of the peak and $\beta_i(2\theta)$ is the measured value of the instrumental line broadening at the same angle 2θ. The crystallite sizes of the powders are presented in Table 1. Addition of NaCl seems to decrease the average crystallite size considerably.

Particle size analysis

The particle size distributions of different samples were determined by using a particle size analyser. The average particle size of sample A, B and C are found to be 11·14, 8·13 and 7·42 μm respectively (Fig. 4). This indicates a decrease in particle size with the addition of NaCl.

Scanning electron microscope

Particle shape analysis is generally one of the most difficult problems in powder technology because there is no general shape factor available that clearly differentiates all possible kinds of shapes.[24]

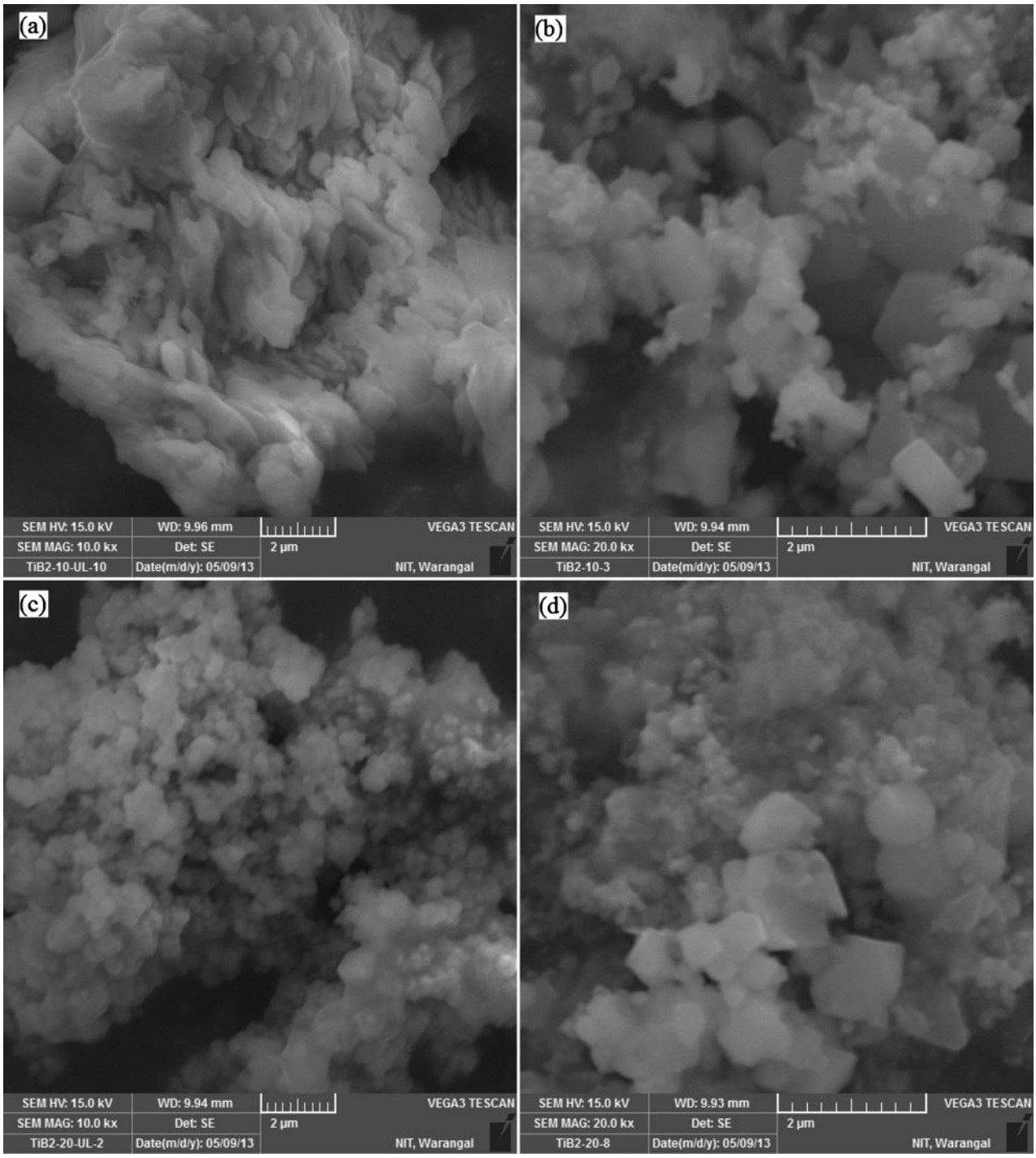

a, *b* unleached and leached powder of sample B (10% NaCl) respectively; *c*, *d* unleached and leached powder of sample C (20% NaCl) respectively

6 Images (SEM) of samples

The SEM images of sample A (0 wt-% NaCl) are shown in Fig. 5. The unleached powder shows presence of agglomeration of spherical particles with the presence of whiskers. There is an active head for the whisker, which indicated the growth of whisker from the head. A similar kind of morphology is noticed during the carbothermal synthesis of boride powder. The mechanism of whiskers formation may be due to vapour–liquid–solid or vapour–solid growth mechanism.[11] The amount of whisker is very less as compared to the spherical particles. However, the presence of whisker is not observed in the leached powder (Fig. 5). The large surface area of whisker leads to sticking to the filter paper, which could not pass through the filter paper during the leaching operation. Presence of agglomeration of particles is observed in the case of leached powder. The morphology of the synthesised powder for sample B and C (10 and 20% NaCl) are shown in Fig. 6. The unleached powder shows agglomeration of fine particles in both the cases whereas leached powder shows particles with variety of shapes such as hexagonal, angular and spherical particles. These powders were further examined under TEM to understand the exact morphology of the powders.

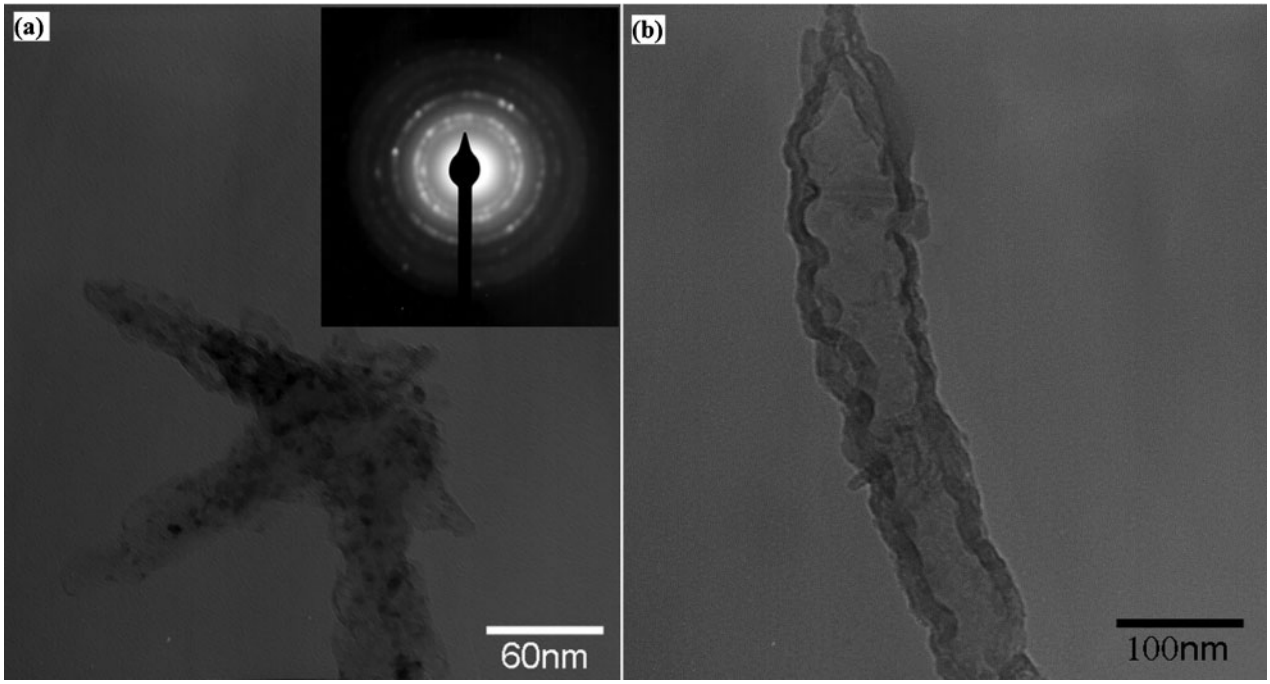

a agglomerate of particles; *b* single rod shaped particle

7 Images (TEM) of leached sample of TiB_2

Transmission electron microscope

The TEM images of leached TiB_2 powder under different processing conditions are shown in Figs. 7–9. The presence of rod shape particles are observed in case of sample A. The morphology of single rod is shown in Fig. 7*b*.The TEM images show the formation of spherical and hexagonal TiB_2 particles, with presence of fibrous structures in the both sample B and C (Figs. 8 and 9). Energy dispersive X-ray spectroscopy analysis of the particles, although not shown in Fig. 9, revealed the Ti enrichment. These results further shows that, after the SHS process, there are formations of both crystalline as well as fibrous structure in the resultant powder. It is found that the TiB_2 powder formed is in the range of 20 to 60 nm and the particle size decreases with the NaCl addition. Figure 8*b, 8c* and 9*b* also show the presence of crystallographic defects such as an array of dislocations, which appear to be formed due to the high cooling rate just after the synthesis. A similar type of morphology was reported by Mishra *et al.*[25]

Role of NaCl

The nature of explosion is much milder in case of NaCl addition and the intensity of explosion decreases with the increasing NaCl. The as synthesised product is found to be lumpy and fragile. The fragility increases with the NaCl addition. The melting and boiling point temperature of NaCl are 810 and 1453°C respectively. The adiabatic temperature of the synthesis is around 2400°C, which indicates during the synthesis some volume fraction of NaCl is vaporised and which may give coating on TiB_2 particles. This coating may results in a decrease in growth rate of particles. Presence of NaCl as a diluent may absorb heat and as a result the adiabatic temperature decreases. This phenomenon indicates that the growth of TiB_2 is occurred at lower temperature with respect to the without addition of salt.

Kinetic study

The XRD pattern of H_3BO_3–Mg system shows presence of MgO as a major phase with Mg in the as synthesised powder (Fig. 10). The XRD pattern of leached powder shows MgB_2 and MgB_4 as a minor phase, respectively. During synthesis of H_3BO_3–Mg system the elemental boron may form, which is not detected by XRD analysis due to amorphous in nature. The XRD pattern of TiO_2–Mg system is shown in Fig. 11. The unleached powder mainly contains MgO and Ti phase, whereas the leached powder shows elemental Ti and TiO_2phase.

Conclusions

The nanocrystalline TiB_2 powder can be produced by SHS process using inexpensive raw materials. The XRD results show the presence of TiB_2 as major phase with TiO_2 (unreacted) as minor phase. The particle size of TiB_2 decreased with the addition of NaCl as SHS diluent. The SEM images show the presence of agglomeration of fine spherical particles. The TEM analysis of the powder reveals that there is a decrease in particle size with the addition of NaCl. The presence of crystallographic defects such as array of dislocations is observed in the synthesised powder.

Acknowledgements

This research work has been funded by the Council of Scientific and Industrial Research (CSIR) (sanction letter no. 22/597/12-EMR-II, dated 2012 March 25). The authors would like to thank Dr Amol A. Gokhale, Director, DMRL and Dr Ghoshal, Group Head, Electron Microcsopy Group, DMRL, for providing permission to carry out TEM investigations.

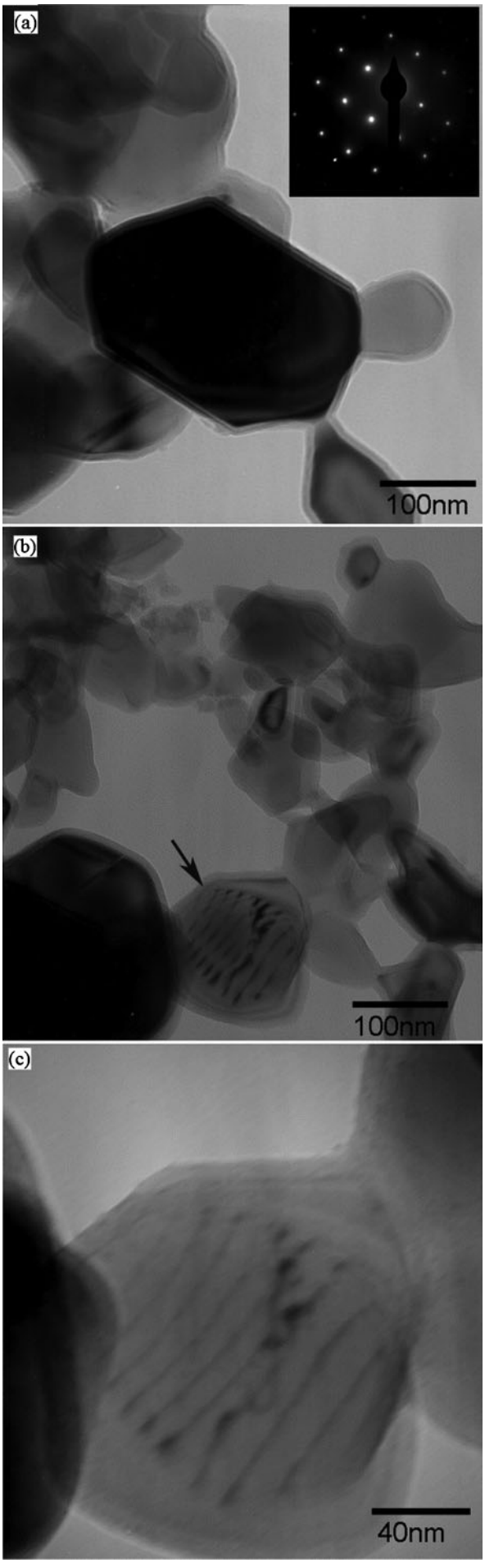

a, *b* BF images showing presence of several TiB_2 particles; *c* high magnification BF image of TiB_2 particle indicated by arrow in *b*

8 Images (TEM) of leached sample of TiB_2 added with 10% NaCl

References

1. U. Demircan, B. Derin and O. Yücel: 'Effect of HCl concentration on TiB_2 separation from a self-propagating high-temperature synthesis (SHS) product', *Mater. Res. Bull.*, 2007, **42**, (2), 312–318.
2. M. Jalaly, M. Sh. Bafghi, M. Tamizifar and F. J. Gotor: 'Mechanosynthesis of nanocrystalline ZrB_2-based powders by mechanically induced self- sustaining reaction method', *Adv. Appl. Ceram.*, 2013, **112**, (7), 383–388.
3. A. W. Weimer: 'Carbide, nitride and boride materials synthesis and processing', 639–651; 1997, London, Chapman & Hall.
4. E. Bilgi, H. Erdem Çamurlu, B. Akgün,Y. Topkaya and N. Sevinç: 'Formation of TiB_2 by volume combustion and mechanochemical process', *Mater. Res. Bull.*, 2008, **43**, 873–881.
5. A. Nekahi and S. Firoozi: 'Effect of KCl, NaCl and $CaCl_2$ mixture on volume combustion synthesis of TiB_2 nanoparticles', *Mater. Res. Bull.*, 2011, **46**, (9), 1377–1383.
6. T. S. Srivatsan, G. Guruprasad, D. Black, R. Radhakrishnan and T. S. Sudarshan: 'Influence of TiB_2 content on microstructure and hardness of TiB_2 – B_4C composite', *Powder Technol.*, 2005, **159**, 161–167.
7. A. Nozari, A. Ataie and S. Karimi: 'Processing of nano-structured TiB_2 by self- propagating high-temperature synthesis (SHS)', *AIP Conf. Proc.* 2012, **382**, 2–6.
8. C. Subramanian, T. S. R. C. Murthy and A. K. Suri: 'Synthesis and consolidation of titanium diboride', *Int. J. Refract. Met. Hard Mater.*, 2007, **25**, (4), 345–350.
9. M. Ziemnicka-sylwester: 'TiB_2-based composites for ultra-high-temperature devices, fabricated by SHS, combining strong and weak exothermic reactions', *Materials*, 2013, **6**, (5), 1903–1919.
10. M. X. Guo, M. P. Wang, K. Shen, L. F. Cao, Z. Li and Z. Zhang: 'Synthesis of nano TiB_2 particles in copper matrix by in situ reaction of double-beam melts', *J. Alloys Compd*, 2008, **460**, (1), 585–589.
11. T. Kühnle and K. Partes: 'In-situ formation of titanium boride and titanium carbide by selective laser melting', *Phys. Proc.*, 2012, **39**, 432–438.
12. A. Calka and D. Oleszak: 'Synthesis of TiB_2 by electric discharge assisted mechanical milling', *J. Alloys Compd*,2007, **440**, (1), 346–348.
13. B. Nasiri-Tabrizi, T. Adhami and R. Ebrahimi-Kahrizsangi: 'Effect of processing parameters on the formation of TiB_2 nanopowder by mechanically induced self-sustaining reaction', *Ceram. Int.*, 2014, **40**, (5), 7345–7354.
14. R. Ricceri and P. Matteazzi: 'Afastandlow-costroomtemperature-process for TiB_2 formation by mechanosynthesis', *Mater. Sci. Eng.*, 2004, **379**, (1), 341–346.
15. D. Y. Kim, Y. J. Lee, T. H. Lee, H. H. Nersisyan, M. H. Han, S. U. Jeong, K. S. Kang, K. K. Bae and J. H. Lee: 'Aluminothermic reduction of K_2TiF_6 to prepare TiC, TiB_2, and TiN nanoparticles', *Combust. Sci. Technol.*, 2014, **186**, (1), 90–101.
16. R. V. Krishnarao and J. Subrahmanyam: 'Studies on the formation of TiB_2 through carbothermal reduction of TiO_2 and B_2O_3', *Mater. Sci. Eng. A*, 2003, **A362**, (1), 145–151.
17. J. W. Kim, J. H. Shim, J. P. Ahn, Y. W. Cho, J. H. Kim, K. H. Oh: 'Mechanochemical synthesis and characterization of TiB_2 and VB_2 nanopowders', *Mater. Lett.* 2008, **62**, 2461–2464.
18. W. M. Tang, Z. X. Zheng, Y. C. Wu, J. M. Wang, J. Lv, J. W. Liu: 'Synthesis of TiB_2 nanocrystalline powder by mechanical alloying', *Trans. Nonferr. Met. Soc.*, 2006, **16**, 613–617.
19. A. Nozari, S. Heshmati-Manesh and A. Ataie: 'A facile synthesis of TiB_2 nano-particles via mechano – thermal route', *Int. J. Refract. Met. Hard Mater.*, 2012, **33**, 107–112.
20. P. Mossino: 'Some aspects in self-propagating high-temperature synthesis', *Ceram. Int.*, 2004, **30**, (3), 311–332.
21. G. H. Liu, J. T. Li and K. X. Chen: 'Review of melt casting of dense ceramics and glasses by high gravity combustion synthesis', *Adv. Appl. Ceram.*, 2013, **112**, (3), 109–124.
22. J. K. Sonber and A. K. Suri: 'Synthesis and consolidation of zirconium diboride: review', *Adv. Appl. Ceram.*, 2011, **110**, (6), 321–334.
23. B. D. Culity: 'Elements of X-ray diffraction', 102–121; 1997, Reading, MA, Addison-Wesley Publishing Company.

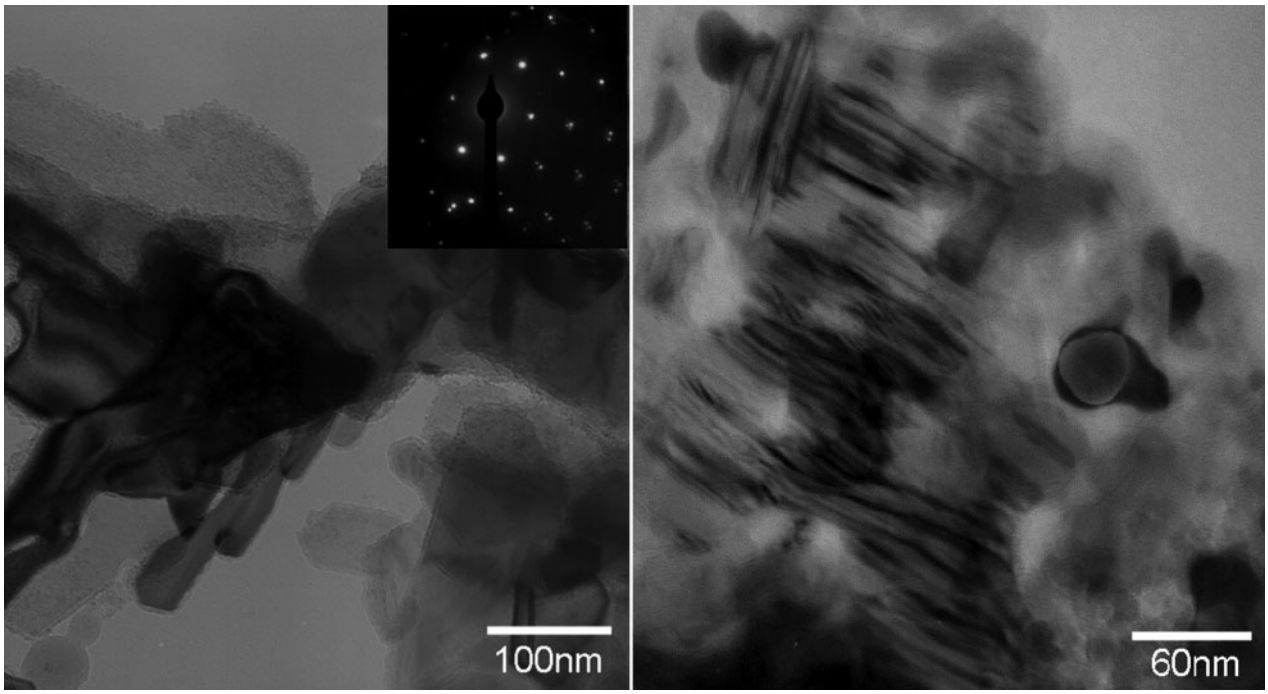

a, *b* BF images

9 Images (TEM) of leached sample of TiB_2 with 20% NaCl

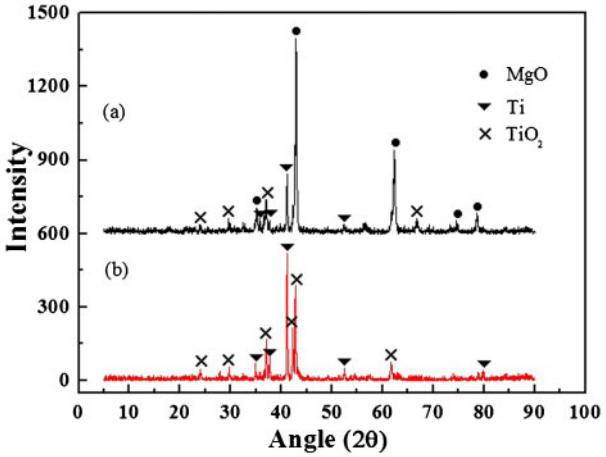

a, *b* unleached and leached powder

10 Patterns (XRD) of TiO_2–Mg system

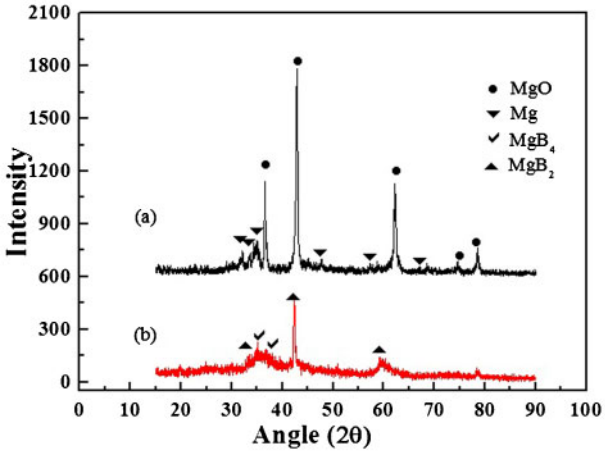

a, *b* unleached and leached powder

11 Patterns (XRD) of H_3BO_3–Mg system

24. P. Pourghahrsamani and E. Forssberg: 'Review of applied particle shape descriptors and produced particle shapes in grinding environments: part 1: particle shape descriptions', *Miner. Process. Extract. Metall. Rev.*, 2005, **26**, 145–166.

25. S. K. Mishra, S. Das and L. C. Pathak: 'Defect structures in zirconium diboride powder prepared by self-propagating high-temperature synthesis', *Mater. Sci. Eng. A*, 2004, **A364**, (1), 249–255.